

The effect of stoichiometry on curing and properties of epoxy–clay nanocomposites

M. A. García del Cid · M. G. Prolongo ·
C. Salom · C. Arribas · M. Sánchez-Cabezudo ·
R. M. Masegosa

MEDICTA2011 Conference Special Chapter
© Akadémiai Kiadó, Budapest, Hungary 2012

Abstract Epoxy–clay nanocomposites have been prepared with an organically modified montmorillonite. The epoxy network was based on diglycidyl ether of bisphenol A (DGEBA) cured with diaminodiphenylmethane (DDM). The stoichiometry DGEBA–DDM was varied, the molar ratio of amine hydrogen/epoxy groups, r , ranged from 0.85 to 1.15. The influence of stoichiometry on curing and properties of the nanocomposites was studied using differential scanning calorimetry, dynamic mechanical thermal analysis and X-ray diffraction. All nanocomposites had intercalated clay structures. The clays accelerated the curing reaction whose rate was also increased when increasing r . The heat of reaction, $-\Delta H$ (J/g epoxy), increased as r increased, reaching a constant value for $r \geq 1$. In the presence of clays $-\Delta H$ was lower than in the neat DGEBA–DDM. The glass transition temperature (T_g) of the neat epoxy thermosets reached a maximum at $r = 1$; however, the nanocomposites showed the T_g maximum at $0.9 < r < 1$. The presence of clay lowered the T_g for $r > 0.94$ and raised T_g for $r \leq 0.85$. The elastic modulus of neat epoxy thermosets reached a maximum in the rubber state and a minimum in the glassy state at $r = 1$. The nanocomposites showed similar behavior, but the maximum and the minimum values of the elastic

modulus were reached at stoichiometry $r < 1$. The comparison of the properties of neat epoxy with those of the nanocomposites varying the stoichiometry indicates that the clay itself induces stoichiometric changes in the system.

Keywords Epoxy–clay nanocomposites · Stoichiometry · Curing · Glass transition · Elastic modulus

Introduction

Polymer–clay nanocomposites are materials obtained by dispersion of clay layers in polymer matrices. The mechanical and thermal properties of nanocomposites are significantly improved, compared with those of neat polymers and conventional composites with similar content of clay [1–5]. The most widely used clay is montmorillonite which is constituted by stacks of layers of 1-nm thick and several hundred nanometers long and wide. Clays are modified by substituting the inorganic cations—which are located between the layers—by alkylammonium cations, to render the clay organophilic [1–4] and therefore compatible with hydrophobic polymers including epoxy thermosets. The nanocomposite morphology may be intercalated, in which the polymer penetrates into the clay galleries, leading to an increase in the clay d -spacing. On the other hand, when the silicate layers are fully dispersed in the polymer matrix, the morphology is named exfoliated [1, 3]. In nanocomposites with fillers having layered structure like clays and graphene, it is of particular interest to achieve exfoliation and total dispersion of the layers, because these structures would present the best properties [1–3, 5–7]. Nevertheless, most of the clay–polymer nanocomposites

M. A. García del Cid · M. G. Prolongo (✉) · C. Salom ·
C. Arribas
Departamento Materiales y Producción Aeroespacial,
Universidad Politécnica de Madrid, Madrid, Spain
e-mail: mg.prolongo@upm.es

M. Sánchez-Cabezudo · R. M. Masegosa
Departamento Física y Química Aplicadas a la Técnica
Aeronáutica, Universidad Politécnica de Madrid, Madrid, Spain

reported in the literature present intercalated structures, and often also present desirable properties [2, 5].

Epoxy–clay nanocomposites have been investigated over the past few years. Although epoxy thermosets have good mechanical and thermal properties, epoxy nanocomposites may enhance the properties even at low nanoparticle contents [5]. To obtain epoxy–clay nanocomposites, the organophilic clay is swollen in the epoxy monomer, after that the curing agent is added and the curing reaction takes place forming the nanocomposite. It is known that the dispersion of nanoparticles in polymers is influenced by the procedure for mixing, specifically, sonication technique may be useful. In epoxy–clay, nanocomposites sonication conduces to disrupt clay agglomerates, but does not give rise to complete dispersion–exfoliation [8, 9]. Actually, it is widely admitted that a main factor for the dispersion of clays in epoxy resins is the balance between intragallery (inside clay layers) and extragallery (outside the clay galleries) cure reactions. Clays modified with alkylammonium cations mainly lead to intercalated structures [5, 9] and in the case of primary alkylammonium cations, the exfoliation is favored, which is attributed to the catalysis of the cure reaction intragallery [10–15].

Epoxy–clay nanocomposites show improvements of the elastic modulus in particular in the rubbery state, that is, at temperatures higher than the glass transition temperature (T_g) [1, 5, 12, 15–18]. However, it is not clear the effect of the clays on the epoxy T_g , both increases and decreases of T_g , has been observed. In rigid epoxies having moderate-high T_g , specifically those cured with aromatic diamines, decreases in the T_g of the epoxy network have been frequently reported [5, 14, 17–19]. This fact has been attributed to the plasticization of the epoxy network by the hydrocarbon chains of the alkylammonium cations [5, 9, 13, 14], besides it has been suggested that the presence of clay may cause stoichiometric imbalances that conduce to the formation of imperfect networks [5, 18, 19]. It is well known that stoichiometry is an important factor in determining the network crosslinking density [20–23] and hence the properties of the thermoset.

The aim of this work is to study off-stoichiometry effects on the curing and on the thermomechanical properties of epoxy–clay nanocomposites with intercalated structures, making a comparison with the neat epoxy thermoset. The stoichiometry diglycidyl ether of bisphenol A–diaminodiphenylmethane (DGEBA–DDM) that is, the molar ratio of amine hydrogen/epoxy groups will be varied and their influence on curing and properties of the nanocomposites will be studied using differential scanning calorimetry (DSC), dynamic mechanical thermal analysis (DMTA) and X-ray diffraction.

Experimental

Materials

The epoxy monomer, DGEBA, was supplied by Uneco S.A. (Spain) under the commercial name of Araldit F. The number average relative molecular mass, $\bar{M}_n = 380 \text{ g mol}^{-1}$, was obtained by chemical titration of the end groups. The curing agent 4,4'-diaminodiphenylmethane (DDM) (97 wt%) was supplied by Sigma-Aldrich Chemical Co. (Spain). We have used two different montmorillonites modified with different alkylammonium cations, although having the same chain length. Organically modified montmorillonites: Cloisite 30B (C30B) and Cloisite 93A (C93A) were supplied by Southern Clay Products, Inc. (Gonzales, TX). Their characteristics: alkylammonium ion, cation exchange capacity (CEC) and interlayer spacing (d_{001}) are given in Table 1. The moisture content of the cloisites is less than 2 wt%. Frekote from Loctite (Spain) was employed as mold release product.

Preparation of the clay dispersions and nanocomposites

Dispersions of clays were prepared by adding the clay powders to the epoxy monomer, stirring at 300 rpm at 120 °C for 2 h. After that, the dispersions appear homogeneous in the polarized optical microscope. The dispersions were degassed for about 15 min under vacuum at 90 °C. Then the curing agent (DDM) was added, and mixed at 80 °C with stirring during 5 min. Finally, the dispersion was sonicated for 2 min. Dispersions having 4 and 6 wt% of clay and neat DGEBA–DDM mixture were prepared. The stoichiometry DGEBA–DDM was varied, the molar ratio of amine hydrogen/epoxy groups, r , ranged from 0.85 to 1.15. To study the curing reaction, small amounts (10–20 mg) of those dispersions and mixtures were poured into aluminum pans, and they were scanned in the differential scanning calorimeter from –50 to 320 °C (curing protocol I), after that, they were rescanned in the DSC to measure the T_g . Moreover, the dispersions were poured into aluminum molds whose walls were previously treated with mold release product, and they were cured in an oven. According to previous works [9, 24], the curing schedule was 120 °C

Table 1 Characteristics of the organically modified montmorillonites

Clay: cloisite	Alkylammonium cation	CEC/meq/100 g	d_{100}/nm
C93A	Methyl, dihydrogenated tallow ^a ammonium	90	2.56
C30B	Methyl, tallow ^a , bis-2-hydroxyethyl quaternary ammonium	90	1.84

^a Tallow ~65% C₁₈, ~30% C₁₆ and ~5% C₁₄

during 2 h, then the temperature was raised to 180 °C (it took about 30 min) and kept at 180 °C for 1 h, under atmospheric pressure (curing protocol II). Specimens having dimensions $35 \times 10 \times 2 \text{ mm}^3$ were cut for DMTA.

Techniques

A Mettler Toledo mod.822e DSC was used to measure the glass transition temperatures and heats of reaction. The instrument was calibrated with indium and zinc, and the measurements were registered at a heating rate of 10 °C/min under nitrogen atmosphere. A M4 Sartorius microbalance was used to weigh the samples of 10–20 mg ($\pm 0.01 \text{ mg}$). Reactive samples show a T_g and an exothermic peak in the first scan, and show only a T_g in the next scans. The T_g 's were taken at the midpoint of the heat capacity change.

DMTA of cured samples under protocol II was performed in dual cantilever bending mode using a DMTA V Rheometric Scientific instrument. Measurements were taken at 1 Hz, with temperature increasing from 30 to 220 °C at a heating rate of 2 °C/min. The elastic storage modulus (E'), the loss modulus (E'') and $\tan\delta$ as a function of temperature were recorded. The maxima in $\tan\delta$ –temperature curves were determined to identify the α -relaxations associated to the glass transitions.

Wide angle X-ray diffraction (WAXD) patterns were obtained at room temperature in reflection mode using a Panalytical X'Pert PRO Alpha1 diffractometer equipped with a curved Ge111 primary beam monochromator and a fast detector X'Celerator (Cu $K\alpha 1$ radiation, $\lambda = 0.15406 \text{ nm}$, 45 kV, 40 mA). The measurement range of 2Θ was from 1.5° to 40°, and step size 0.0167°.

Results and discussion

Dynamic curing of DGEBA–clay dispersions by DSC

First of all, dispersions of clays in DGEBA were prepared without adding curing agent, and they were scanned in the DSC to check the reactivity of the system. Figure 1 shows the DSC curves (first scans) of the clay dispersions together with the scan of neat DGEBA. In all cases, a glass transition was observed around -16 °C that corresponds to the initial un-reacted epoxy resin. It was followed by an exothermal peak that corresponds to the epoxy homopolymerization (see Scheme 1) [10]. This exothermal peak appears at lower temperatures when the clays are present indicating their catalytic effect over the homopolymerization. It can be seen that C93A favors the epoxy homopolymerization more than C30B. The second scans only showed a T_g around 88 °C that is associated to the epoxy homopolymer (polyether).

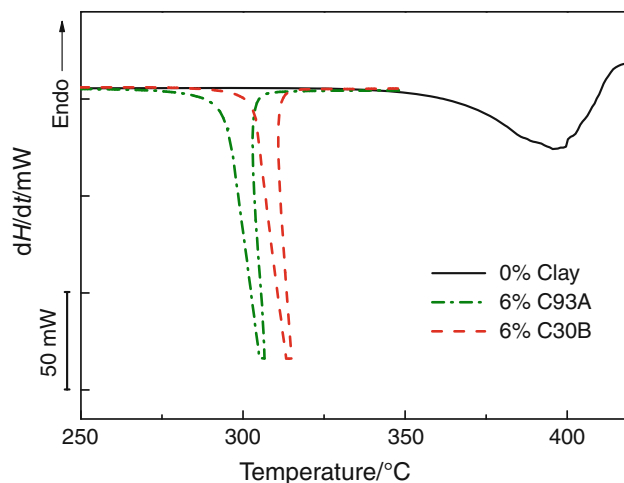


Fig. 1 DSC curves of neat DGEBA (straight line) and of the dispersions having 6 wt% of clay: DGEBA–C93A (dashed spaced line) and DGEBA–C30B (dashed line)

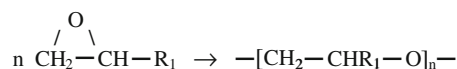
Dynamic curing of DGEBA–DDM–clay dispersions by DSC

The curing of dispersions of DGEBA–DDM–clay and of DGEBA–DDM mixtures having different stoichiometries was studied by DSC. Figure 2 shows the DSC curves for dispersions of C30B and C93A in the stoichiometric mixture DGEBA–DDM ($r = 1$). In all cases, a glass transition is observed around -12 °C ; this T_g that corresponds to the un-reacted mixture is followed by a single exothermal peak of the curing reaction (see Scheme 1). The addition of clay shifts the exothermal peak at lower temperatures, thus the curing DGEBA–DDM reaction is accelerated in the presence of C93A or C30B. Similar behavior, that is, a catalytic effect of the organically modified clay, has been reported for other epoxy–clay systems [5, 9, 14, 18, 25]. In the systems here studied the acidic alkylammonium cations in C93A and the hydroxyl groups of the alkylammonium cations of C30B catalyze epoxy homopolymerization and epoxy–diamine reaction [10–15]. The curing study of the off-stoichiometric mixtures reveals similar catalytic clay effect, as it is illustrated in Fig. 3, which shows the peak temperature (T_{peak}) dependence with the stoichiometry: For each r value, the T_{peak} of the neat DGEBA–DDM is higher than for clay–DGEBA–DDM dispersion. Moreover, it can be seen that T_{peak} decreases as r increases, that is, as the amine content increases. This behavior has been observed in other DGEBA–diamine systems [26], and it would be a consequence of the self-dilution effect of the reactants and catalytic effects of amine groups.

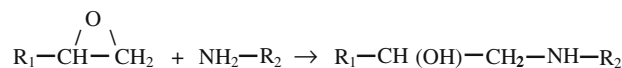
The heats of reaction ($-\Delta H$) have been calculated from the exothermal peak areas (from 50 to 260 °C), and they are given as J/g of epoxy (DGEBA). Figure 4 shows the dependence of $-\Delta H$ on stoichiometry. As expected,

Scheme 1 Epoxy homopolymerization, epoxy-amine and epoxy-OH reactions

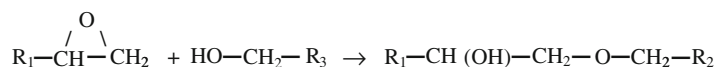
Epoxy homopolymerization:



Epoxy-amine reaction:



Epoxy-OH reaction:



$-\Delta H$ reaches a constant value for $r \geq 1$ (excess of amine groups), since all the epoxy groups have reacted. Also it can be seen that $-\Delta H$ is lower in the presence of clays than in the neat DGEBA-DDM, but at $r = 0.85$ (excess of DGEBA) the differences disappear. This suggests that the clays may have induced changes in stoichiometry. DGEBA and DDM could have been intercalated in different extension within the clay galleries, leading to stoichiometric imbalances which would reduce $-\Delta H$. The changes in stoichiometry due to the clays are in agreement with previous results that correlate $-\Delta H$ with the clay content [9]. As the clays were swollen in DGEBA, it is expected that DGEBA molecules were preferentially intercalated into the clay. Therefore, there would not have enough DDM to completely react with DGEBA intragallery, and the DGEBA excess intragallery would not contribute to $-\Delta H$. It can be deduced that the $-\Delta H$ values for DGEBA-DDM and for DGEBA-DDM-clay dispersions will coincide from one composition, r' ($r' < 1$) in which the amount of unreacted DGEBA intragallery coincides with the excess of DGEBA corresponding to r' with respect to $r = 1$. It can be noticed in Fig. 4 that r' value is $r = 0.85$.

It is worthy to note that when curing with DDM, the homopolymerization of the DGEBA is not likely for $r \geq 1$. DGEBA-DDM reaction is significantly faster than epoxy homopolymerization, thus homopolymerization would only occur when DGEBA is in excess ($r < 1$) [27, 28]. In the DSC experiments (see Fig. 2), homopolymerization reaction was not detected, only for $r = 0.85$, a small exothermal peak was observed but at higher temperatures (300–320 °C) for C93A and for C30B dispersions.

Glass transitions of epoxy-clay nanocomposites

To analyze the effects of the clay and of the stoichiometry over the T_g of the cured epoxy networks two types of samples were prepared: samples cured during the DSC scan from -50 to 320 °C at 10 °C/min (protocol I) and samples cured in an oven: 2 h at 120 °C + 1 h at 180 °C (protocol

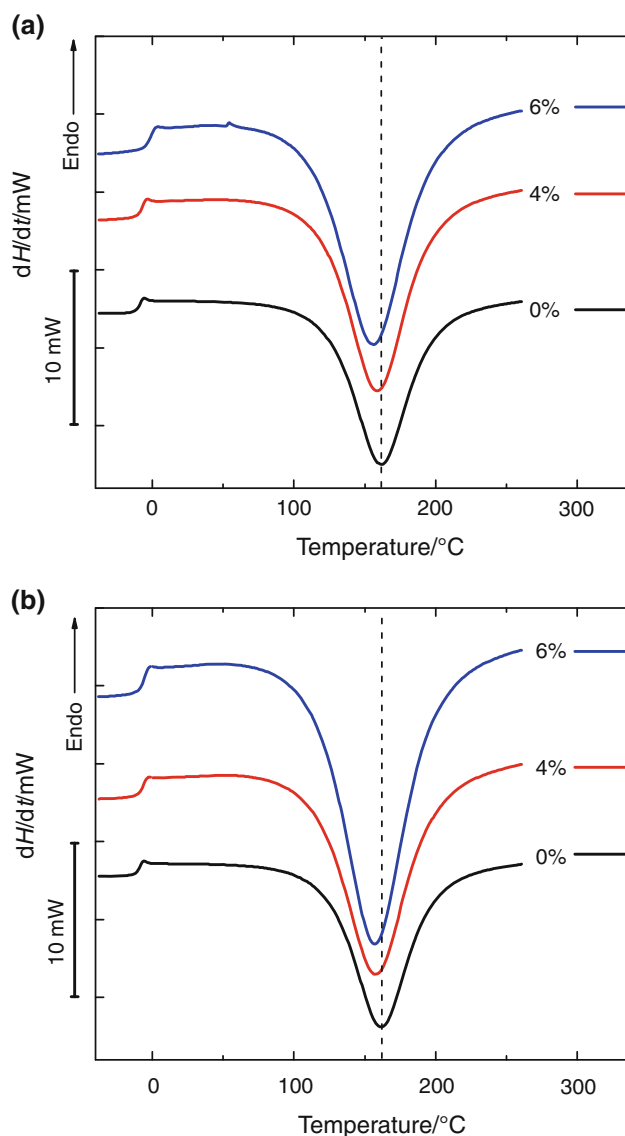


Fig. 2 DSC curves of the dynamic curing of: **a** DGEBA-DDM-C93A dispersions and **b** DGEBA-DDM-C30B dispersions, having different clay contents: 0 wt% (straight line), 4 wt % (straight line) and 6 wt% (straight line)

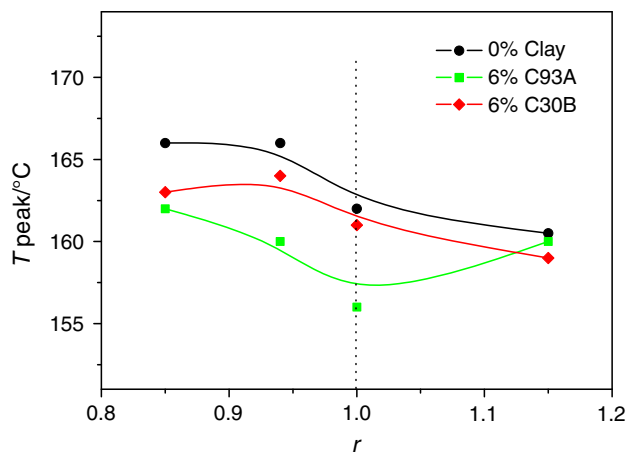


Fig. 3 T_{peak} of dynamic curing as a function of stoichiometry for DGEBA–DDM (circle) and for the dispersions having 6 wt% of clay: DGEBA–DDM–C93A (square) and DGEBA–DDM–C30B (diamond)

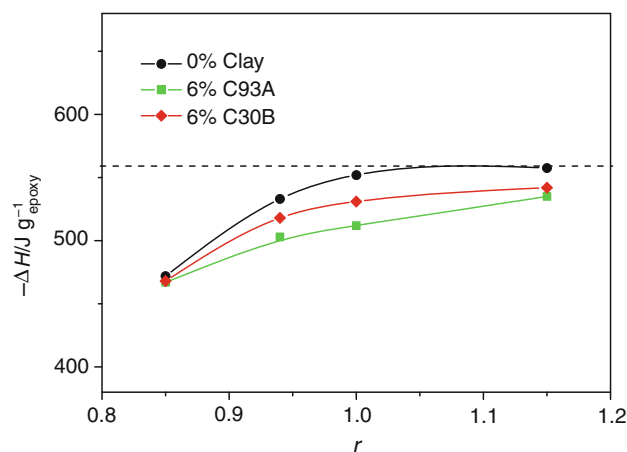


Fig. 4 $-\Delta H$ (kJ/g epoxy) as a function of stoichiometry for DGEBA–DDM (circle) and for the dispersions having 6 wt% of clay: DGEBA–DDM–C93A (square) and DGEBA–DDM–C30B (diamond)

II). After being cured, the samples were scanned in the DSC, in all the cases, only a single T_g was observed, which corresponds to the cured epoxy network. Both types of samples present similar T_g values indicating that both curing protocols give rise to similar network structures. Figure 5 shows the dependence of T_g with the stoichiometry, in the epoxy–clay nanocomposites and in neat epoxy thermosets, which have been cured during the DSC scan. As it can be seen the T_g values depend strongly on the stoichiometry. It is well known that the crosslinking density of epoxy–amine thermosets is highly affected by the stoichiometry, and the highest crosslinking density is obtained at the stoichiometric composition [20–23]. The off-stoichiometry leads to network structures having lower crosslinking density and therefore, lower T_g than the

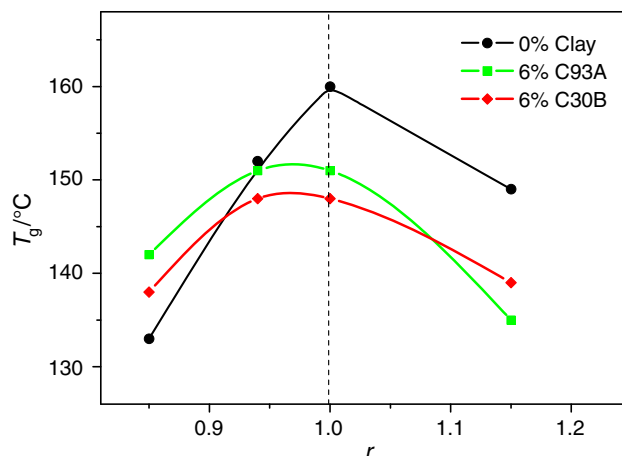


Fig. 5 T_g as a function of stoichiometry for DGEBA–DDM thermoset (circle) and for the nanocomposites containing 6 wt% of clay: DGEBA–DDM–C93A (square) and DGEBA–DDM–C30B (diamond). Samples cured during the DSC scan

stoichiometric mixture. The epoxy–clay nanocomposites also show a strong dependence of T_g with the stoichiometry (Fig. 5), the presence of clay decreases the T_g at $r > 0.94$, but T_g increases if $r \leq 0.85$, and the maximum T_g is obtained for $0.94 \leq r < 1$. This behavior will be analyzed below together with $\tan\delta$ results obtained from DMTA.

WAXD of epoxy–clay nanocomposites

To analyze the influence of the clays on the T_g of the epoxy network, the structure of the nanocomposites should be known. Figure 6 shows the WAXD patterns of epoxy–clay nanocomposites together with those of neat clays. The neat C93A shows an intense peak at $2\theta = 3.45^{\circ}$ that corresponds to an interlayer distance: $d_{001} = 2.56$ nm. The neat C30B shows an intense peak at $2\theta = 4.79^{\circ}$ that corresponds to an interlayer distance: $d_{001} = 1.84$ nm. The nanocomposites show diffraction peaks at lower values, the peaks at $2\theta \sim 2.6^{\circ}$ correspond to interlayer distances of $d_{001} \sim 3.4$ – 3.5 nm which are higher than in neat clays. This indicates that nanocomposites are intercalated, since exfoliated nanocomposites show absence of peaks in WAXD pattern, ($1.5^{\circ} < 2\theta < 10^{\circ}$) and d -spacing of at least 6 nm [5, 14]. The organophilic nature of the cloisites makes it possible for epoxy monomers to access into the clay galleries [1–3] pushing the silicate layers apart and forming intercalated structures. The increments of interlayer distances, Δd_{001} , are 1.6 nm for epoxy–C30B nanocomposites and 0.9 nm for epoxy–C93A nanocomposites, hence it seems that epoxy molecules intercalate in a greater extension in C30B than in C93A. It is interesting to notice that both cloisites reach in the nanocomposites similar interlayer spacing. As the alkyl chain lengths of the ammonium cations are similar for both clays, this indicates

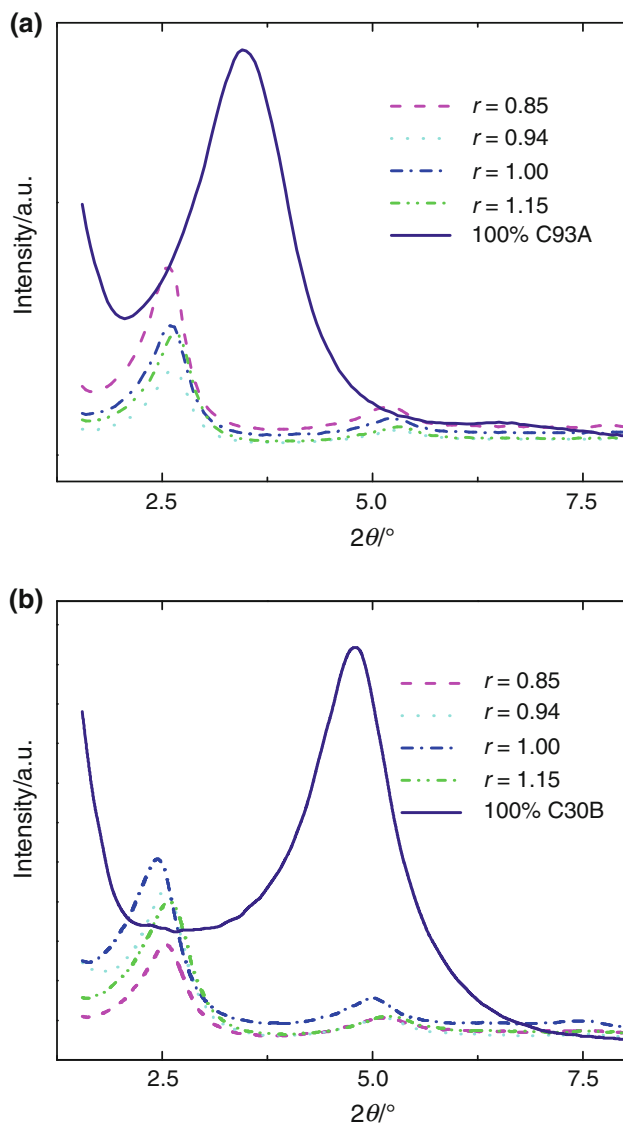


Fig. 6 WAXD patterns of: **a** pristine C93A and DGEBA-DDM-C93A nanocomposites containing 6 wt% of clay with different stoichiometry, **b** Pristine C30B and DGEBA-DDM-C30B nanocomposites containing 6 wt% of clay with different stoichiometry

a similar arrangement of the alkylammonium cations within the gallery space. This is consistent with a layer of inclined alkylammonium ions that have been reoriented into the clay gallery forming a paraffin-type layer that permits to accommodate the epoxy molecules [1, 2, 4].

Dynamic mechanical properties of epoxy-clay nanocomposites

DMTA measurements of samples of epoxy thermoset and epoxy-clay nanocomposites having different stoichiometry, cured under protocol II, were carried out. As an example, Fig. 7 illustrate the $\tan\delta$ -temperature dependence for the neat epoxy thermoset and epoxy-clay

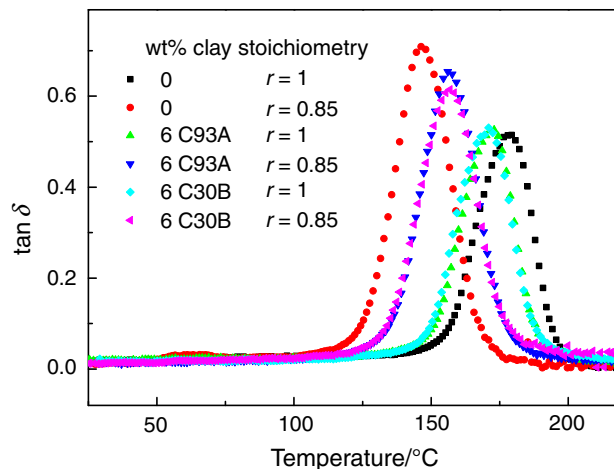


Fig. 7 $\tan\delta$ -temperature dependence for DGEBA-DDM-C93A and DGEBA-DDM-C30B nanocomposites containing 6 wt% of clay and for DGEBA-DDM thermoset, with stoichiometry: $r = 1$ and $r = 0.85$

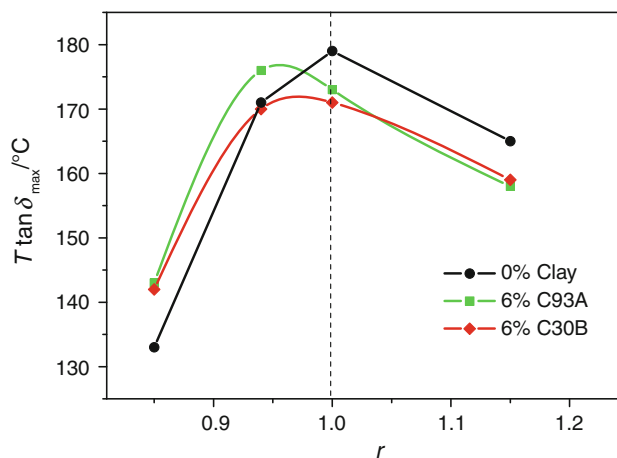


Fig. 8 Temperature of $\tan\delta$ peak as a function of stoichiometry for DGEBA-DDM-C93A (square), DGEBA-DDM-C30B (diamond) nanocomposites containing 6 wt% of clay and for DGEBA-DDM thermoset (circle)

nanocomposites with $r = 1$ and $r = 0.85$. The $\tan\delta$ peak is the α -relaxation associated to the glass transition; the temperature of the maximum at 1 Hz is taken as a measure of T_g ; their values are higher than the ones determined by DSC [29].

Figure 8 displays the temperature of $\tan\delta$ peak ($T_{\tan\delta \text{ peak}}$) as a function of the stoichiometry for all the compositions studied. As expected, Figs. 5 and 8 show similar behavior. Neat epoxy thermoset shows a maximum $T_{\tan\delta \text{ peak}}$ (maximum T_g) value for the stoichiometric composition ($r = 1$), that is, the network having the highest crosslinking density. The nanocomposites show similar behavior, but the maximum T_g is displaced to $r < 1$ ($0.94 \leq r < 1$). In comparison with the neat epoxy

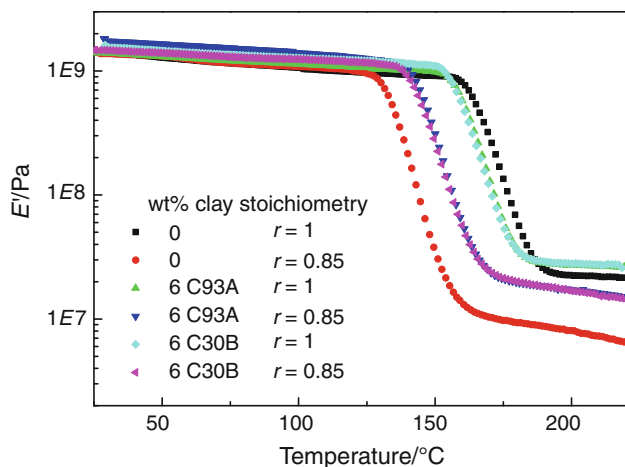


Fig. 9 E' -temperature dependence for DGEBA–DDM–C93A, DGEBA–DDM–C30B nanocomposites containing 6 wt% of clay and for DGEBA–DDM thermoset, with stoichiometry: $r = 1$ and $r = 0.85$

thermoset, the nanocomposites show lower T_g for $r > 0.9$. Two effects may contribute to lowering the epoxy T_g : the plasticizing effect of the epoxy network by the alkylammonium chains [5, 9, 13, 14] and imbalances of stoichiometry [5, 18, 19]. As we have discussed above, C93A and C30B nanocomposites present intercalated structures, although the values of Δd_{001} indicate that epoxy molecules intercalate in higher extension in C30B than in C93A, the C93A has two long alkyl chains that will provide more free volume in the interaction with the epoxy network, thus the plasticizing effect of C93A and C30B may not be so different. The plasticizing effect of the alkylammonium cations could explain that the nanocomposites do not reach the T_g value of the neat epoxy thermoset with stoichiometric composition ($r = 1$), which has the highest T_g . However, it does not explain the displacement of the maximum in T_g to lower r in the nanocomposites.

A lower T_g means that the segmental mobility of the network increases, thus the second effect that would contribute to the decrease of the T_g would be the lowering of the epoxy crosslinking density. In intercalated nanocomposites, the lowering of crosslinking density may be originated by imbalances of stoichiometry, as a consequence of preferential intercalation of DGEBA molecules. The T_g – r trend of epoxy–C30B y epoxy–C93A nanocomposites is similar. C30B and C93A induce changes in stoichiometry that conduce to form networks of highest T_g and highest crosslinking density for off-stoichiometric composition close to $r \sim 0.94$. On the other hand, for $r = 0.85$, the T_g values of nanocomposites are higher than the T_g value of the neat epoxy thermoset. In the samples with excess of DGEBA, it is expected that DGEBA homopolymerization and the reaction between hydroxyl groups of the epoxy network and epoxy groups (see Scheme 1) take

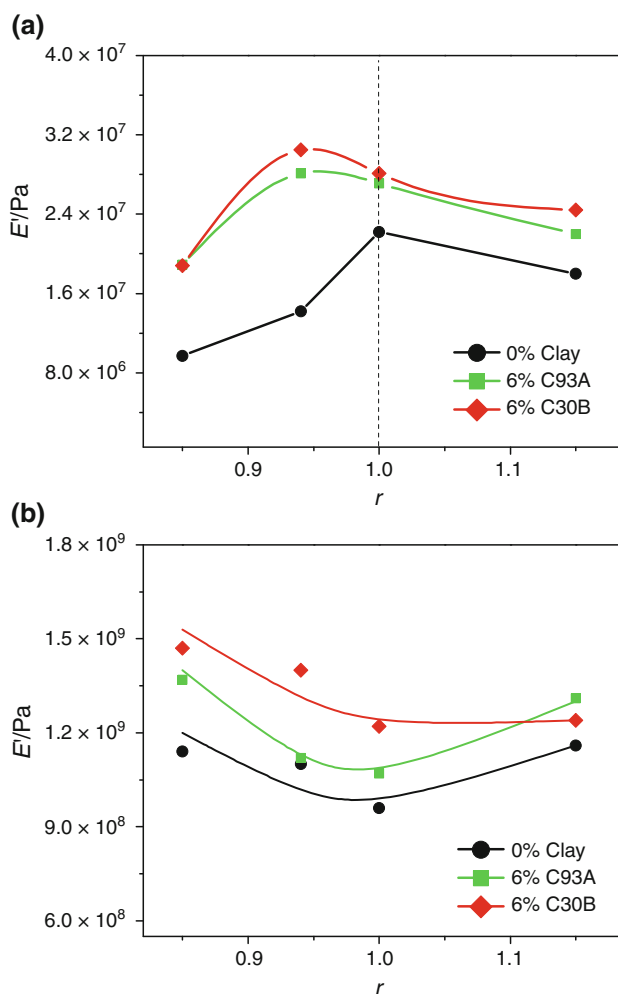


Fig. 10 E' as a function of stoichiometry for DGEBA–DDM–C93A (square), DGEBA–DDM–C30B (diamond) nanocomposites containing 6 wt% of clay, and for DGEBA–DDM thermoset (circle): **a** rubber state ($T_g + 30$ °C) and **b** glassy state ($T_g - 50$ °C)

place in the presence of the clays [10, 12, 27]. These reactions may explain the raising of the T_g respect to neat epoxy thermoset at $r = 0.85$. Samples cured under protocol I were heated to 320 °C and those cured under protocol II were heated at 180 °C long time, these conditions favor both reactions, thus Figs. 5, 8 show similar behavior.

A study of the influence of stoichiometry on epoxy–carbon nanotube nanocomposites has been done simultaneously to this work [30]. The behavior of the neat epoxy system is similar to ours. However, the effect of carbon nanotubes on the epoxy T_g is different, specifically, for $r > 1$, the epoxy–carbon nanotube nanocomposites show higher T_g than the neat epoxy thermoset. The different behavior of epoxy–clay nanocomposites at $r > 1$ must be caused by the intercalation into clay layers as it was above discussed.

Figure 9 shows E' -temperature dependence for the neat epoxy thermoset and epoxy–clay nanocomposites with

$r = 1$ and $r = 0.85$. As can be seen the elastic storage modulus in the rubbery state ($T > T_g$) is increased with the presence of clay, this also occurs in the glassy state ($T < T_g$) although it is not well appreciated in the figure. The values of E' in the glassy state (taken at $T_g - 50$ °C) and in the rubber state (taken at $T_g + 30$ °C) are plotted as a function of the stoichiometry in Fig. 10. The rubber modulus is a measure of the crosslinking density of a polymer network. Neat epoxy thermosets in the rubbery state present the highest modulus for the stoichiometric sample (see Fig. 10a) which has the highest crosslinking density and the highest T_g . However, in the glassy state, the stoichiometric sample presents the lowest modulus (see Fig. 10b) this behavior is well known [20–23], and it is explained as a consequence of low molecular packing and the influence of the β -relaxation of the epoxy that occurs at around -50 °C, which is minimized in non-stoichiometric systems [10–23]. Epoxy–C93A and epoxy–C30B nanocomposites have higher elastic modulus than the neat epoxy thermoset, both in the glassy state and in the rubber state. In nanocomposites in the rubber state, the maximum value of E' is reached at $r = 0.94$ that coincides with the stoichiometry at which the T_g reaches the maximum value.

Conclusions

Epoxy–clay nanocomposites with organically modified montmorillonites: cloisites C93A and with C30B (4–6 wt% clay content) were prepared. The stoichiometry of the epoxy (DGEBA–DDM) was varied, the molar ratio of amine hydrogen/epoxy groups, r , ranged from 0.85 to 1.15. The nanocomposites have intercalated clay structures, being the interlayer clay spacing almost independent on the clay and on stoichiometry. The increments of d -spacing in nanocomposites indicate that the epoxy molecules intercalate in higher proportion in C30B than in C93A.

The effect of the clays on the curing reaction has been studied by DSC. The clays accelerate the curing reaction, due to the catalytic effect of the alkylammonium cations. The curing rate was also increased when increasing r , due to a catalytic effect of the amine excess. As expected the heat of reaction, $-\Delta H$, expressed as J/g epoxy, increased with increasing r and reached a constant value for $r \geq 1$; moreover, $-\Delta H$ is lower in the presence of clays than in the neat DGEBA–DDM for $r \geq 0.9$, this is attributed to stoichiometric imbalances induced by the clay. The coincident $-\Delta H$ values obtained at $r = 0.85$ for neat epoxy thermoset and nanocomposites indicate that the amount of unreacted DGEBA intragallery coincides with the excess of DGEBA in $r = 0.85$.

The glass transition temperature of the neat epoxy thermosets reaches a maximum at $r = 1$, but the

nanocomposites show the maximum at $r \sim 0.9$, this is attributed to stoichiometric imbalances caused by the clays. The T_g s of nanocomposites having $r = 0.85$ are higher than the T_g of the neat epoxy thermoset, this is related to the reactions of the excess of DGEBA (homopolymerization and epoxy–hydroxyl) that take place in the presence of the clays and contribute to increase the crosslinking density.

The plasticizing effect of the alkylammonium cations could explain that the neat epoxy thermoset with stoichiometric composition has the highest T_g , and that the nanocomposites do not reach that value at any stoichiometry.

The elastic modulus of neat epoxy thermosets reaches at $r = 1$ a maximum in the rubber state and a minimum in the glassy state. The nanocomposites showed similar behavior but the minimum and maximum are located at stoichiometry $r < 1$.

As a main conclusion, all these results indicate that in epoxy–clay nanocomposites having intercalated structures, the clays induce stoichiometric imbalances that can explain the changes in T_g and modulus of these materials.

Acknowledgements Financial support by Ministerio de Educación y Ciencia of Spain (MAT 2009-11083) and by Universidad Politécnica de Madrid-Investigation Groups Support is acknowledged.

References

1. LeBaron PC, Wang Z, Pinnavaia TJ. Polymer-layered silicate nanocomposites: an overview. *Appl Clay Sci.* 1999;15:11–29.
2. Pavlidou S, Papispyrides CD. A review on polymer-layered silicate nanocomposites. *Prog Polym Sci.* 2008;33:1119–98.
3. Paul DR, Robeson LM. Polymer nanotechnology: nanocomposites. *Polymer.* 2008;49:3187–204.
4. Betega de Paiva LB, Morales AR, Valenzuela-Díaz FR. Organoclays: properties, preparation and applications. *Appl Clay Sci.* 2008;42:8–24.
5. Becker O, Simon GP. Epoxy layered silicate nanocomposites. *Adv Polym Sci.* 2005;179:29–82.
6. Qiu J, Wang S. Enhancing polymer performance through graphene sheets. *J Appl Polym Sci.* 2011;119:3670–4.
7. Potts JR, Dreyer DR, Bielawski CW, Ruoff RS. Graphene-based polymer nanocomposites. *Polymer.* 2011;52:5–25.
8. Nuhiji B, Attard D, Thorogood G, Hanley T, Magniez K, Fox B. The effect of alternate heating rates during cure on the structure-property relationships of epoxy/MMT clay nanocomposites. *Compos Sci Technol.* 2011;71:1761–8.
9. Prolongo MG, Martínez-Casado FJ, Masegosa RM, Salom C. Curing and dynamic mechanical thermal properties of epoxy/clay nanocomposites. *J Nanosci Nanotechnol.* 2010;10:2870–9.
10. Lan T, Kaviratna PD, Pinnavaia TJ. Epoxy self-polymerization in smectite clays. *J Phys Chem Solids.* 1996;57:1005–10.
11. Wang Z, Pinnavaia TJ. Hybrid organic-inorganic nanocomposites: exfoliation of magadiite nanolayers in an elastomeric epoxy polymer. *Chem Mater.* 1998;10:1820–6.
12. Messersmith PB, Giannelis EP. Synthesis and characterization of layered silicate–epoxy nanocomposites. *Chem Mater.* 1994;6:1719–25.

13. Triantafyllidis CS, LeBaron PC, Pinnavaia TJ. Thermoset epoxy–clay nanocomposites: the dual role of α,ω -diamines as clay surface modifiers and polymer curing agents. *J Solid State Chem.* 2002;167:354–62.
14. Park J, Jana SC. Effect of plasticization of epoxy networks by organic modifier on exfoliation of nanoclay. *Macromolecules.* 2003;36:8391–7.
15. Brown JM, Curliss D, Vaia RA. Thermoset-layered silicate nanocomposites. Quaternary ammonium montmorillonite with primary diamine cured epoxies. *Chem Mater.* 2000;12:3376–84.
16. Lan T, Pinnavaia TJ. Clay-reinforced epoxy nanocomposites. *Chem Mater.* 1994;6:2216–9.
17. Hussain F, Chen J, Hojjati M. Epoxy–silicate nanocomposites: cure monitoring and characterization. *Mater Sci Eng A.* 2007;467:445–6.
18. Nigam V, Setua DK, Mathur GN, Kar KK. Epoxy–montmorillonite clay nanocomposites: synthesis and characterization. *J Appl Polym Sci.* 2004;93:2201–10.
19. Garea S, Iovu H, Stoleriu S, Voicu G. Synthesis and characterization of new nanocomposites based on epoxy resins and organophilic clays. *Polym Int.* 2007;56:1106–14.
20. Gupta VB, Drzal LT, Lee CY. The temperature-dependence of some mechanical properties of a cured epoxy resin system. *Polym Eng Sci.* 1985;25:812–23.
21. Palmese GR, McCullough RL. Effect of epoxy–amine stoichiometry on cured resin material properties. *J Appl Polym Sci.* 1992;46:1863–73.
22. Meyer F, Sanz G, Eceiza A, Mondragon I, Mijovic J. The effect of stoichiometry and thermal history during cure on structure and properties of epoxy networks. *Polymer.* 1995;36:1407–14.
23. Munz M, Sturm H, Stark W. Mechanical gradient interphase by interdiffusion antiplasticisation effect-study and epoxy/thermoplastic system. *Polymer.* 2005;46:9097–112.
24. Sánchez-Cabezudo M, Prolongo MG, Salom C, Masegosa RM. Cure kinetics of epoxy resin and thermoplastic polymer. *J Therm Anal Calorim.* 2006;86:699–705.
25. Román F, Montserrat S, Hutchinson JM. On the effect of montmorillonite in the curing reaction of epoxy nanocomposites. *J Therm Anal Calorim.* 2007;1:113–8.
26. Zvetkov VL, Krastev RK, Samichkov VI. Rate equations in the study of the DSC kinetics of epoxy–amine reactions in an excess of epoxy. *Thermochim Acta.* 2008;478:17–27.
27. Sherman LC, Zeigler RC, Verghese NE, Marks MJ. Structure–property relationships of controlled epoxy networks with quantified levels of excess epoxy etherification. *J Polymer.* 2008;49:1164–72.
28. Macan J, Brnardic I, Ivancovic M, Mencer HJ. DSC study of cure kinetics of DGEBA-based epoxy resin with poly(oxypropilene) diamine. *J Therm Anal Calorim.* 2005;81:369–73.
29. Sánchez-Cabezudo M, Masegosa RM, Salom C, Prolongo MG. Correlations between the morphology and the thermo-mechanical properties in poly(vinyl acetate)/epoxy thermosets. *J Therm Anal Calorim.* 2010;102:1025–33.
30. Gude MR, Prolongo SG, Ureña A. Effect of the epoxy/amine stoichiometry on the properties of carbon nanotube/epoxy composites. *J Therm Anal Calorim.* 2011. doi:[10.1007/s10973-011-2056-x](https://doi.org/10.1007/s10973-011-2056-x).